Journal of Hazardous Materials 189 (2011) 150–157

Contents lists available at ScienceDirect

Journal of Hazardous Materials

journal homepage: www.elsevier.com/locate/jhazmat

The effect of Nd on the properties of ceria–zirconia solid solution and the catalytic performance of its supported Pd-only three-way catalyst for gasoline engine exhaust reduction

Qiuyan Wang[a], Guangfeng Li[a], Bo Zhao[a,b], Renxian Zhou[a,*]

[a] Institute of Catalysis, Zhejiang University, 148 # Tianmushan Road, Hangzhou 310028, PR China
[b] School of Pharmaceutical and Chemical Engineering, Taizhou University, Taizhou 317000, PR China

ARTICLE INFO

Article history:
Received 25 October 2010
Received in revised form 1 February 2011
Accepted 6 February 2011
Available online 2 March 2011

Keywords:
$Ce_{0.2}Zr_{0.8}O_2$
Neodymia
Oxygen storage capacity
Thermal stability
Pd-only three-way catalyst

ABSTRACT

A series of ceria–zirconia–neodymia mixed oxides with different contents of neodymia and the supported Pd-only three-way catalysts before and after aging have been prepared and characterized. The influence of Nd doping on the structural/textural properties of ceria–zirconia (CZ) and the effect on the three-way catalytic performance are also investigated. The results demonstrate that the addition of neodymia results in the formation of ceria–zirconia–neodymia ternary solid solution (CZN) with better textural and structural properties as well as improved reducibility and redox behavior, leading to the promoted three-way catalytic activity and enlarged air/fuel operation window. The modified solid solution with 5 wt.% neodymia shows the preferable textural/structural properties considering that the capacity of foreign cation is limited in the crystal lattice of ceria–zirconia solid solution, and Pd/CZN5 shows the optimum three-way catalytic performance and wider air/fuel operation window, especially for the corresponding aged one.

1. Introduction

Air pollution mainly caused by exhausts from gasoline engine powered vehicles is one of the major environmental concerns and has drawn more and more attention in recent years [1,2]. Among the several techniques that have been developed for reducing gasoline engine exhaust, catalytic converter is regarded as the most promising solution [3–7]. As the key component in catalytic converter, three-way catalyst (TWC) has been successfully used for the control and suppression of automotive emission by converting basic air pollutants like carbon monoxide, hydrocarbons and nitrogen oxides simultaneously. Along with the more rigorous environmental regulations imposed on the automobile industry, more efficient TWC is required.

In the actual formulations of TWC, Pd exhibit excellent capability for low-temperature oxidation of carbon monoxide and hydrocarbons compared with Pt and Rh-supported catalysts [8,9]. On the other hand, Pd is relatively economical and abundant than Pt and Rh, especially than Rh. Therefore, Pd-only TWC has received considerable attention. Ceria–zirconia solid solution is widely employed as a promoter in TWC, and it represents the state-of-art of the so-called oxygen storage materials (OSM) [10–16]. Ceria–zirconia solid solution shows large concentration of surface and bulk oxygen-vacant sites, the fast exchange of surface oxygen with gas-phase oxygen species and the high diffusion rates of bulk oxygen towards its surface, all due to the presence of a rapid Ce^{3+}/Ce^{4+} redox couple. These important features, named oxygen storage capacity (OSC), provide a way to minimize fluctuation of the air-to-fuel (A/F) ratio at around 14.6 during engine operation. Under the transitions between lean and rich operating conditions, ceria–zirconia material stores or releases oxygen, thus ensuring that TWC work effectively within a narrow operating window near the stoichiometric A/F ratio [12,17–19].

In practice, the demand for decrease of cold-start emissions requires the catalyst to be located in positions closer to the engine manifold, where the temperature can rise even above 1000 °C [10,20–22]. As it is well-known, the exposure of catalysts to that high temperature will induce the sintering of both ceria–zirconia solid solution and active noble metal, causing the loss of OSC and the deactivation of TWC. Consequently, one of the recent requirements for developed TWC is the higher OSC and thermal stability under high temperature conditions. Until now, a great deal of research attention has been paid to the intrinsic structure and properties of ceria–zirconia solid solution [13–15,23–26], and it was found that the incorporation of other rare earth elements [2,7,27–31] is beneficial to increase the OSC and improve the thermal stability of ceria–zirconia mixed oxides. Nevertheless, summarizing the literature, the mechanism over these promoted properties of rare

* Corresponding author. Tel.: +86 571 88273290; fax: +86 571 88273283.
E-mail address: zhourenxian@zju.edu.cn (R. Zhou).

0304-3894/$ – see front matter.
doi:10.1016/j.jhazmat.2011.02.012

Table 1
Light-off temperature ($T_{50\%}$) and full-conversion temperature ($T_{90\%}$) of HC, CO, NO and NO_2 over all the fresh catalysts.

Sample	$T_{50\%}$ (°C)				$T_{90\%}$ (°C)			
	HC	CO	NO	NO_2	HC	CO	NO	NO_2
Pd/CZ	229	158	231	180	263	191	264	214
Pd/CZN3	226	167	210	174	257	199	263	205
Pd/CZN5	218	184	206	170	254	202	244	195
Pd/CZN8	224	186	188	165	255	205	224	185
Pd/CZN10	227	188	187	160	257	209	223	179

earth modified ceria–zirconia solid solution remains obscure, and research related to the effect of rare earth doping on the catalytic activity of TWC is little.

This work deals with a combined investigation of the effect of Nd doping on the structural/textural properties of ceria–zirconia solid solution and on the three-way catalytic performance of its supported Pd-only catalyst. A series of $Ce_{0.2}Zr_{0.8}O_2$ (CZ) modified with different neodymia contents were prepared and characterized by techniques such as X-ray diffraction (XRD), N_2 adsorption/desorption and X-ray photoelectron spectroscopy (XPS). The redox properties and OSC of the materials were studied by means of hydrogen temperature-programmed reduction (H_2-TPR), H_2–O_2 and CO–O_2 pluses. The catalytic activity of TWC was evaluated under the simulative automobile exhaust and the air/fuel ratio experiments were also carried out.

2. Experimental

2.1. Catalyst preparation

CZ and Nd modified CZ (CZN) supports were prepared by conventional coprecipitation method combined with supercritical drying technique. The detailed procedure was similar to literature [32]. The molar ratio of Ce:Zr is 1:4, and the additive content of neodymia is 3, 5, 8 and 10 wt.% for CZN, respectively. The fresh supports calcined at 500 °C are named as CZN*x* (*x* = 3, 5, 8, 10), where *x* means the content of neodymia. All the supports were also calcined at 1100 °C for 4 h to investigate the effect of doping on the thermal stability of CZ, and the aged supports are referred to as CZa and CZNxa, respectively. The corresponding Pd/CZ and Pd/CZN*x* catalysts were prepared by wet impregnation method. The as-received fresh catalysts were aged at 1100 °C for 4 h to investigate the thermal stability. The theoretical loading content of Pd for all the catalysts is 0.5 wt.%. The catalysts obtained at 1100 °C are labeled as Pd/CZa and Pd/CZNxa, respectively.

2.2. Catalytic activity test

The evaluation of three-way catalytic activity was performed on a Bruker EQ55 FTIR spectrometer coupled with a multiple reflection transmission cell (Infrared Analysis Inc.). The detailed information was also shown in [32].

The air/fuel ratio (λ) experiments were carried out at 400 °C. λ is defined as $(2V_{O_2} + V_{NO} + 2V_{NO_2})/(V_{CO} + 9V_{C_3H_6} + 10V_{C_3H_8})$ [32] (*V* means concentration in volume percent unit), and λ = 1 was used in all the activity measurements. The test of air/fuel operation window was carried out at λ = 0.9, 0.92, 0.95, 0.98, 1.0, 1.04, 1.07, 1.1 and 1.15, respectively [33–35].

2.3. Characterization techniques

The X-ray photoelectron spectroscopy (XPS) experiments were carried out on a PHI-Quantera SXM system equipped with a monochromatic Al Kα X-rays under ultra-high vacuum (6.7×10^{-8} Pa). Sample charging during the measurement was compensated by an electron flood gun. The XPS data from the regions related to C 1s, O 1s, Zr 3d, Ce 3d, Pr 3d and Pd 3d core levels were recorded for each sample. The binding energies were calibrated internally by the carbon deposit C 1s binding energy (BE) at 284.8 eV. The deconvolution method of XPS spectra is fitted by Gaussian function.

The oxygen storage capacity complete (OSCC) was measured using pulse injection technique with a CHEMBET-3000. The sample was first reduced with a flow of 10 ml/min H_2 at 550 °C for 1 h, then cooled to the testing temperature and purged by helium stream. The OSCC was measured by pulse injection of oxygen into the sample bed until no consumption of oxygen could be detected by TCD. The amount of oxygen consumed during the re-oxidation stage is referred as OSCC. All the gases employed in the experiment were high-purity (99.999%).

In addition, the characterization related to powder X-ray diffraction (XRD), N_2 adsorption/desorption, H_2-temperature programmed reduction (H_2-TPR) and dynamic oxygen storage capacity (DOSC) were also carried out according to the methods reported in literature [32].

3. Results and discussion

3.1. Catalytic performance

All the fresh and aged catalysts were evaluated in the simulative gasoline engine exhaust and the tail gas after reaction was detected by FTIR. The light-off temperature ($T_{50\%}$, the temperature at which 50% conversion is attained) and full-conversion temperature ($T_{90\%}$, the temperature at which 90% conversion is attained) of HC, CO, NO and NO_2 over all the fresh catalysts were summarized in Table 1. As reported in literature [9], the main chemical reactions taking place during the automobile exhaust treatment is as following:

Oxidation:

$$2CO + O_2 \rightarrow 2CO_2$$

$$HC + O_2 \rightarrow CO_2 + H_2O \quad \text{(unbalanced reaction)}$$

Reduction:

$$2CO + 2NO \rightarrow 2CO_2 + N_2$$

$$HC + NO \rightarrow CO_2 + H_2O + N_2 \quad \text{(unbalanced reaction)}$$

$$2H_2 + 2NO \rightarrow 2H_2O + N_2$$

Water–gas shift:

$$CO + H_2O \rightarrow CO_2 + H_2$$

Steam reforming:

$$HC + H_2O \rightarrow CO_2 + H_2 \quad \text{(unbalanced reaction)}$$

From Table 1, it can be known that the introduction of Nd promotes the catalytic conversion of both NO and NO_2 obviously, the $T_{50\%}$ and $T_{90\%}$ of which decrease clearly with the increasing amount

Table 2
Light-off temperature ($T_{50\%}$) and full-conversion temperature ($T_{90\%}$) of HC, CO, NO and NO_2 over all the aged catalysts.

Sample	$T_{50\%}$ (°C)				$T_{90\%}$ (°C)			
	HC	CO	NO	NO_2	HC	CO	NO	NO_2
Pd/CZa	372	265	386	315	423	305	443	383
Pd/CZN3a	340	259	347	275	367	279	398	324
Pd/CZN5a	307	254	316	263	345	270	348	310
Pd/CZN8a	333	226	330	220	361	242	363	260
Pd/CZN10a	337	218	335	216	363	234	366	250

of neodymia. This observation indicates that the addition of Nd is beneficial to the reduction in the process of three-way catalytic reaction for the fresh catalysts. On the contrary, the appearance of Nd shows an inhibiting effect on CO elimination considering that the $T_{50\%}$ and $T_{90\%}$ of CO increase with the increasing neodymia content over all the fresh catalysts. In the case of HC catalytic conversion, only slight promotion was observed for the Nd modified samples.

Table 2 shows the results of catalytic conversion of HC, CO, NO and NO_2 over all the aged catalysts. According to the values of $T_{50\%}$ and $T_{90\%}$ in Table 2, all the aged samples doped with Nd are active in enhancing the catalytic activity for all the target pollutants. For HC and NO conversion, an improvement is observed with increasing Nd doping content from 3 wt.% to 5 wt.%, whereas a decline is obtained by further increasing the loading amount to 8 wt.% and 10 wt.%, signifying that the catalytic activity of HC and NO over Pd/CZN5a is the highest among all the aged catalysts. With regard to the catalytic conversion of CO and NO_2, the $T_{50\%}$ and $T_{90\%}$ of the aged catalysts decrease clearly with the increasing Nd amount, proving the increased catalytic activity due to the addition of Nd.

The difference of $T_{50\%}/T_{90\%}$ between the fresh and corresponding aged catalyst is labeled as $\Delta T_{50\%}/\Delta T_{90\%}$, which are presented in Table 3. A remarkable drop of catalytic activity is observed from the increased $T_{50\%}$ and $T_{90\%}$ when comparing with the relevant fresh catalysts, which can be ascribed to the deteriorated structure and the sintering of active component arising from the high-temperature treatment [1,14]. For example, both the light-off temperature and full-conversion temperature of HC, CO, NO and NO_2 over Pd/CZa goes up more than 100 °C. In general, $\Delta T_{50\%}$ and $\Delta T_{90\%}$ can be a measure of thermal stability of the catalysts. As shown in Table 3, the value of $\Delta T_{50\%}$ and $\Delta T_{90\%}$ for all the pollutants over the modified catalysts are lower than Pd/CZ, which indicates that the addition of Nd to the support is beneficial to increase the thermal stability of the corresponding catalyst.

Fig. 1 presents the results of air/fuel (λ) test over all the fresh and aged catalysts. As shown in Fig. 1, the left side of the theoretical stoichiometric value ($\lambda = 1.0$) is the lean oxygen condition and the right is rich oxygen condition. From Fig. 1 it can be seen that in the case of the fresh catalysts, the conversion of HC achieves 100% in the whole air/fuel testing range. The CO conversion increases with the increasing O_2 content and it approaches 100% at $\lambda = 0.95$ over Pd/CZN5, Pd/CZN8 and Pd/CZN10, while at $\lambda = 1.0$ over Pd/CZN3 and Pd/CZ. One thing should be mentioned is that the conversion of CO over the fresh catalyst is higher than 85% even though under the so-called lean oxygen condition. In addition, all the fresh catalysts show 100% conversion of CO under the rich oxygen condition. It is evident that the width of CO operation window follows the sequence of Pd/CZN5 > Pd/CZN8 > Pd/CZN10 > Pd/CZN3 > Pd/CZ (shown in Fig. 1B). Under the lean oxygen condition, the conversion of NO_x is 100%. Instead, it decreases clearly with the increasing O_2 content under the rich oxygen condition. Similarly to CO conversion, Pd/CZN5 shows the widest NO_x operation window. After being aged at high temperature, the operation window of all the catalysts is destroyed greatly. The conversion of HC and NO_x over Pd/CZa is lower than 80% in the whole air/fuel testing range, and the conversion of CO only achieves 100% at the theoretical stoichiometric. However, the operation window of HC, CO and NO_x is enlarged obviously due to the presence of Nd, and the width of the operation window has a degressive trend of Pd/CZN5a > Pd/CZN8a > Pd/CZN10a > Pd/CZN3a > Pd/CZa. Based on the analysis mentioned above, a main point can be put forward that all the modified catalysts are more active in three-way catalytic conversion, and the addition of Nd with optimum content leads to the obviously improved catalytic activity, thermal stability and enlarged operation window of the supported Pd-only three-way catalyst.

3.2. Structural and textural properties

XRD patterns of the fresh and aged supports are presented in Fig. 2. The BET surface area, the lattice parameters and the crystal size for all the supports are summarized in Table 4. The lattice parameters were derived from a Rietveld refinement of XRD results and the corresponding crystal size was calculated according to Scherer equation. All the fresh supports exhibit only peaks which could be referred to the tetragonal ceria–zirconia solid solution (space group $P_{42}/nmcs$, $Z = 2$, ICSD No. 68590), and separated neodymia phases are not observed for the four Nd modified supports. As shown in Fig. 2A, the reflections are quite broad and symmetrical for all the fresh samples, indicating the formation of fine nanostructure [7]. After treatment at 1100 °C for 4 h, the reflections of the aged supports become sharper and more intense when comparing with the fresh one, indicating the occurrence of obvious sintering. This observation agrees well with the increased crystalline size as depicted in Table 4. In the case of CZa and CZN3a, the separation of peaks around 35°, 58° and 72° takes place, although

Table 3
The change of light-off temperature ($T_{50\%}$) and full-conversion temperature ($T_{90\%}$) of HC, CO, NO and NO_2 over catalysts before and after aged.

Sample	$\Delta T_{50\%}$ (°C)				$\Delta T_{90\%}$ (°C)			
	HC	CO	NO	NO_2	HC	CO	NO	NO_2
Pd/CZ	143	106	155	135	160	114	179	169
Pd/CZN3	114	92	137	101	110	80	135	119
Pd/CZN5	89	70	110	93	91	68	104	115
Pd/CZN8	109	40	142	55	106	37	139	75
Pd/CZN10	110	30	148	56	106	25	143	71

$\Delta T_{50\%} = T_{50\%}$ (aged catalyst) − $T_{50\%}$ (fresh catalyst).
$\Delta T_{90\%} = T_{90\%}$ (aged catalyst) − $T_{90\%}$ (fresh catalyst).

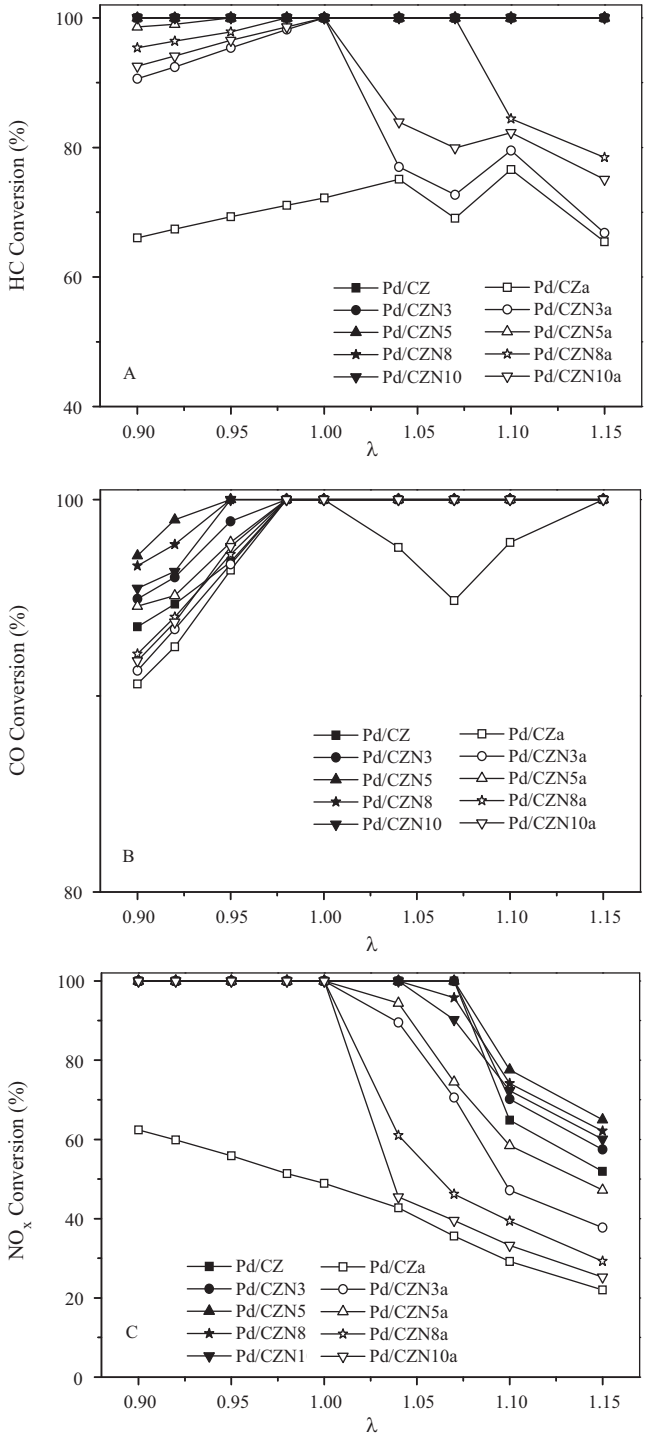

Fig. 1. Conversion curves of HC, CO and NO_x as a function of air/fuel ratio (λ) over the fresh and aged catalysts.

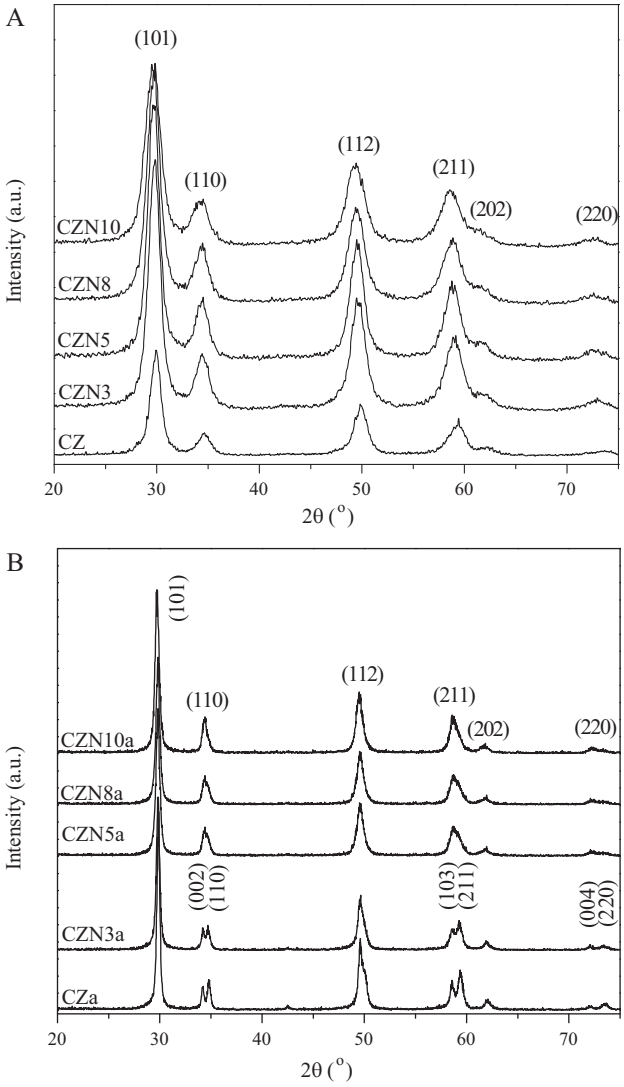

Fig. 2. XRD patterns of fresh (a) and aged (b) supports.

all of these peaks are also consistent with tetragonal ceria–zirconia solid solution. Moreover, a careful investigation of the XRD patterns in Fig. 2B shows that degree of splitting for CZN3a is lower than CZa. Interestingly, no additional peaks are observed at CZN5a, CZN8a and CZN10a, and no distinct difference could be seen among the XRD patterns of them. The observation presented above indicates that the sintering for the aged supports is clearly attenuated with the increasing neodymia content, and the further modification is absent once the content of neodymia is enough.

Table 4 shows that the lattice parameter for all the Nd doped samples is larger than that of CZ, which indicates the expansion of lattice, proving the formation of Ce–Zr–Nd ternary solid solution [36,37]. The ionic radius of Nd^{3+} (1.00 Å) is larger than Zr^{4+} (0.84 Å),

Table 4
BET surface area, lattice constants, crystallite size and OSCC of samples.

Samples	Surface area (m^2/g)	Lattice constants (Å)	Crystallite size (Å)	OSCC (μmol[O_2]/g)
CZ	105.9/24.3[a]	a = 3.625/3.632[a], c = 5.218/5.227[a]	6.7/32.2[a]	265/282
CZN3	115.6/26.6[a]	a = 3.656/3.648[a], c = 5.204/5.235[a]	5.7/25.0[a]	316/347
CZN5	127.1/28.8[a]	a = 3.655/3.648[a], c = 5.217/5.224[a]	5.1/17.2[a]	338/385
CZN8	130.2/29.3[a]	a = 3.680/3.672[a], c = 5.219/5.233[a]	5.1/14.9[a]	334/363
CZN10	130.5/30.8[a]	a = 3.684/3.683[a], c = 5.230/5.223[a]	4.9/14.4[a]	321/354

[a] BET surface area, lattice constants, crystallite size and OSCC for the aged samples.

Table 5
Surface composition and surface atom ratio in the representative fresh and aged catalysts derived from XPS analyses.

Sample	Surface composition (at.%)					Zr/Ce	Ce^{3+} $3d_{5/2}$ in Ce (%)
	Ce 3d	Zr 3d	Nd 3d	Pd 3d	O 1s		
Pd/CZ	2.88	13.68	0	–	83.44	4.75	17.29
Pd/CZN5	2.84	13.41	0.09	–	83.66	4.72	19.64
Pd/CZa	3.42	12.23	0	0.04	84.31	3.58	15.21
Pd/CZN5a	3.75	11.69	0.18	0.02	84.36	3.12	17.04

and the radius of Ce^{3+} and Ce^{4+} is 1.14 Å and 0.97 Å, respectively. Firstly, the substitution of Ce^{3+} by Nd^{3+} is unbelievable, for it would lead to the lattice shrinkage. Secondly, the ionic radius of Ce^{4+} is close to Nd^{3+}. Although Ce^{4+} could be substituted by Nd^{3+}, the amount must be very little for it cannot account for the obviously lattice expansion. On the other hand, the amount of Ce in the lattice is relatively low considering it is Zr-rich solid solution (the theoretical molar ratio of Ce to Zr is 1:4). Therefore, the cation site substitution of Zr by Nd seems more credible. Table 4 also shows that for the fresh supports, the grain size is obviously decreased with the increase of neodymia loading content, and no clear decline can be observed when the content of neodymia increases from 5 wt.% to 10 wt.%. The same behavior also happens to the aged supports. This observation demonstrates that the optimum loading content of neodymia is 5 wt.%, considering that the capacity of foreign cation is limited in the crystal lattice of ceria–zirconia solid solution.

From Table 4, it can be seen that all the Nd doped fresh supports show higher specific surface area than CZ, suggesting that the presence of Nd results in the improved textural stability of CZ solid solution. A clearly defined decrease in BET surface area is observed when comparing the aged supports with the fresh ones, which stems from the sintering effects. However, the aged samples doped with Nd also show higher specific surface area than CZa. Interestingly, for both the fresh and aged supports, the specific surface area increases with the loading amount of neodymia increases from 3 wt.% to 5 wt.%, and no obvious increase occurs when the content increases from 5 wt.% to 10 wt.%, indicating that Nd modified supports with 5 wt.% loading content shows the preferable thermal stability again.

3.3. XPS results

XPS was conducted to investigate the effect of neodymia addition on the oxidation state of Ce and on the surface elemental distribution of the catalysts. The Ce 3d spectra over Pd/CZ, Pd/CZN5, Pd/CZa and Pd/CZN5a are illustrated in Fig. 3. The surface elemental compositions of the catalysts calculated from the normalized peak areas of the Ce 3d, Zr 3d, Nd 3d, Pd 3d and O 1s core level spectra are summarized in Table 5.

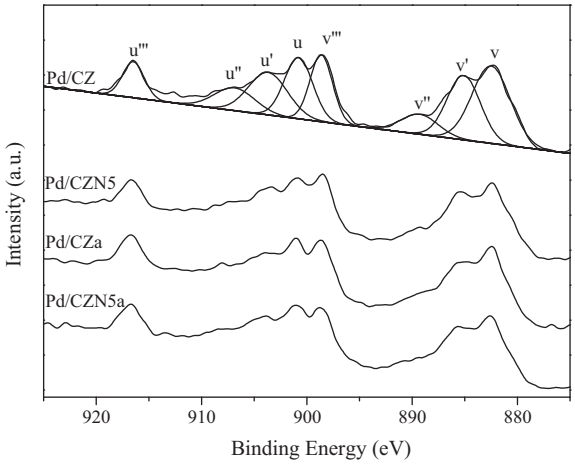

Fig. 3. Ce 3d spectra for Pd/CZ, Pd/CZN5, Pd/CZa and Pd/CZN5a.

The curve of Ce 3d spectra shown in Fig. 3 comprises eight peaks corresponding to four pairs of spin–orbit doublets. Early studies [38–40] have shown that Ce $3d_{3/2}$ multiplets are labeled as u, whereas those of $3d_{5/2}$ are labeled as v. Specifically, the peaks marked as u, u'' and u''' arise from Ce^{4+} $3d_{3/2}$ while the peaks denoted as v, v'' and v''' arise from Ce^{4+} $3d_{5/2}$, the couples corresponding to one of the two possible electron configuration of the final state of the Ce^{3+} species are labeled as u' and v'. The relative percentages of cerium species are obtained by the area ratios of Ce^{4+} $3d_{5/2}$ (v, v'' and v''')/Ce^{3+} $3d_{5/2}$ (v'). From Table 5, it can be known that the Nd doped samples show higher relative concentration of Ce^{3+} than Pd/CZ. Summarizing the literature [38,41], it is generally recognized that the presence of Ce^{3+} is associated with the formation of oxygen vacancies according to the electroneutrality condition. Therefore, we can conclude that the introduction of Nd into CZ solid solution increases the oxygen vacancies on the surface of sample.

In the XPS experiment, no Pd is observed in the case of the fresh catalysts. On the one hand, the loading content of Pd is extremely low, which approaches the limit detection (0.5 wt.%). On the other hand, Pd appeared on the surface of the catalysts may be highly dispersed. However, Pd is detectable in the case of aged catalysts, indicating the obvious sintering of noble metal due to the high temperature treatment. Moreover, the surface content of Nd for the Pd/CZN5a is apparently higher than Pd/CN5, indicating the enrichment of Nd on the surface of supports due to the calcination at 1100 °C for 4 h. What should be mentioned is that the content of Pd on the surface of Pd/CZN5a is 0.02 at.%, which is half that of Pd/CZa. This observation implies that the addition of Nd would improve the strong metal-support interaction (SMSI), inhibiting the sintering of noble metal on the interface of support. A perusal of the results from Table 5 shows that the surface atom ratios of Zr/Ce over Pd/CZN5 and Pd/CZN5a are slightly smaller than those over Pd/CZ and Pd/CZa, which means that part of Zr atoms of the surface layer is replaced by Nd.

3.4. Redox behavior

Strong oxygen storage ability and good redox behavior would render a TWC well behaved under oscillatory reaction conditions. The H_2–O_2 and CO–O_2 titration as well as TPR methods were adopted to probe the oxygen storage capability and the redox behavior of the samples.

3.4.1. OSC measurement

The OSCC data for the fresh and aged supports tested at 400 °C are shown in Table 4. For both the fresh and aged supports, the Nd doped samples have a higher OSCC than CZ/CZa, indicating that the incorporation of Nd^{3+} into lattice of CZ strongly favors creation of structural defects and results in the acceleration of oxygen diffusion [2]. Moreover, Table 4 also shows that the OSCC value increases with increasing Nd doping content from 3 wt.% to 5 wt.%, whereas a decline is obtained by further increasing the loading amount to

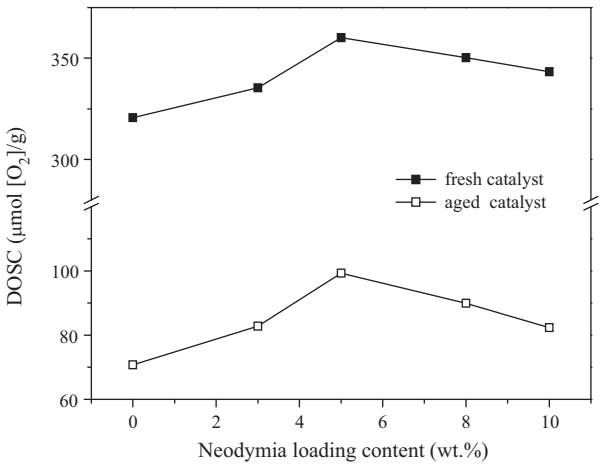

Fig. 4. The DOSC value for the fresh and aged catalysts.

8 wt.% or 10 wt.%, signifying that the OSCC of CZN5 is the highest among the fresh supports. As reported in the literatures [12,42–45], the OSC of ceria–zirconia is intrinsic to its structure. The more homogeneous structure increases the oxygen vacancies relating to the structure modification which results in the promotion of OSC [42], indicating that CZN5 exhibits the most homogenous structure.

A careful comparison of the OSCC data reveals that the aged sample exhibits slight higher OSCC than the corresponding fresh one. For the fresh samples, the OSCC is mostly related to the surface labile oxygen species [17]. With regard to the aged support, the BET surface area experiences a sharply decline, and the amount of surface available oxygen species is lower, which cannot afford the higher OSCC of the aged samples. The most reasonable explanation could be that the increase of calcination temperature promotes the presence of "less reducible" oxygen species and results in the enhanced mobility of bulk oxygen, which is the main contributor to OSCC of the aged supports [17,31].

The data of DOSC for the fresh and aged catalysts are shown in Fig. 4. The greatest amount of DOSC is produced at sample with 5 wt.% neodymia content no matter before or after aged, and the presence of Nd also results in an increased DOSC than the undoped sample, which is consistent with the result of the H_2–O_2 pulse injection technique. After calcination at 1100 °C for 4 h, the DOSC value of aged catalyst is decreased obviously compared with the corresponding fresh one. For the fresh catalysts, the results of DOSC agree well with OSCC of the corresponding supports, indicating that there is marginal difference on the status of active PdO among the fresh catalysts. Combined with the fact that the OSCC is enhanced after calcination, it can be concluded that the main reason for the dramatic decline of DOSC is the agglomeration of active PdO species caused by sintering effect [46].

3.4.2. H_2 temperature-programmed reduction (H_2-TPR)

The reducibility of supported TWCs is an important factor influencing its catalytic performance and H_2-TPR is a common technique to investigate the reducibility of samples [47–49]. The results of consecutive TPR profiles of the supports and the catalysts are presented in Figs. 5 and 6, respectively. Fig. 5A shows that all the fresh supports exhibit one dominant broad peak with maxima at ca. 570 °C and several minor peaks in the range of low temperature. The previous literatures [10,50] have reported that two peaks at about 500 and 800 °C are found in the TPR profile of ceria–zirconia mixed oxide, which are associated with the reduction at the surface and in the bulk. Therefore, all the peaks appear in the case of fresh supports is more likely to be related to the reduction of surface oxygen. Moreover, it can be seen from Fig. 5A that the reduction

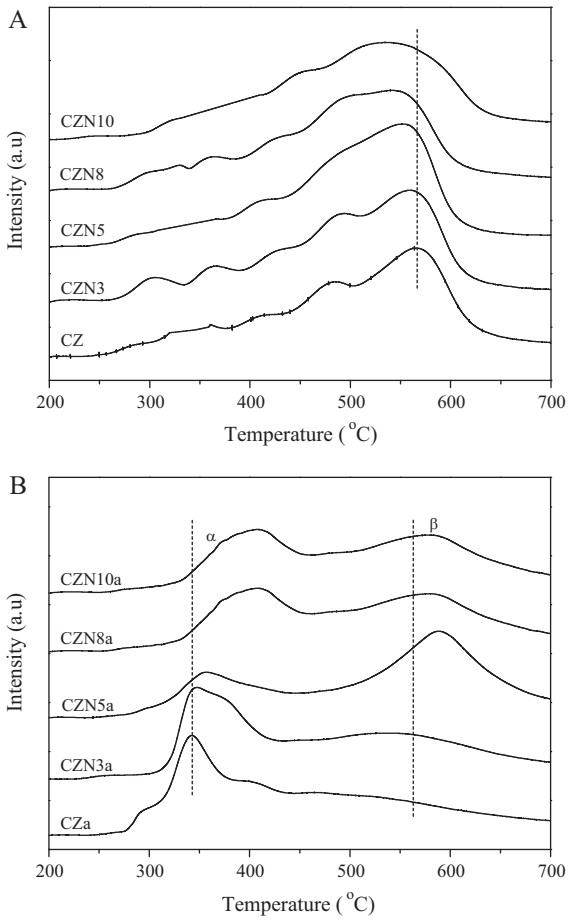

Fig. 5. TPR traces for the fresh and aged supports.

already started at ca. 250 °C, indicating the good reducibility of the samples in this paper. An interesting feature of these profiles is that all the Nd doped samples shows lower peak temperature than CZ, proving that the addition of Nd results in the enhanced reducibility of CZ.

Comparison of the TPR profiles between aged supports and the fresh ones shows that the thermal aging induces significant changes of the reduction behavior for the supports. As illustrated in Fig. 5B, two main reduction peaks are observed. The peak located at relatively lower temperature is denoted as peak α and the other one is labeled as peak β, which are ascribed to the reduction of surface and sub-surface oxygen [18,33,51], respectively. The splitting of surface oxygen into separated surface and sub-surface oxygen indicates that the declined homogeneity of the fresh supports due to calcination at 1100 °C for 4 h. The most significant change of the TPR behavior before and after aged occurs in CZa and CZN3a, especially for CZa. For CZa and CZ3a, the symmetry of peak α is poor and the intensity of peak β is very weak. The most possible reason is the obvious deteriorated structure during the high temperature treatment, which has been testified by the XRD patterns of the aged supports.

Fig. 6 shows the TPR responses of catalysts before and after aging. For the fresh catalysts, all of the samples exhibit a strong low-temperature reduction feature at ca. 65 °C (peak α). Previous investigations have reported that palladium oxide is reduced to palladium on exposure to H_2 at room temperature [52,53]. In addition, no characterization is observed below 150 °C in the TPR profiles of fresh supports (Fig. 5A), which further proved that peak α could be mainly attributed to the reduction of PdO species. The tiny peaks in the range of 150–400 °C are also associated with the reduction of surface oxygen [31,32,46]. Based on the amount of H_2 consumption

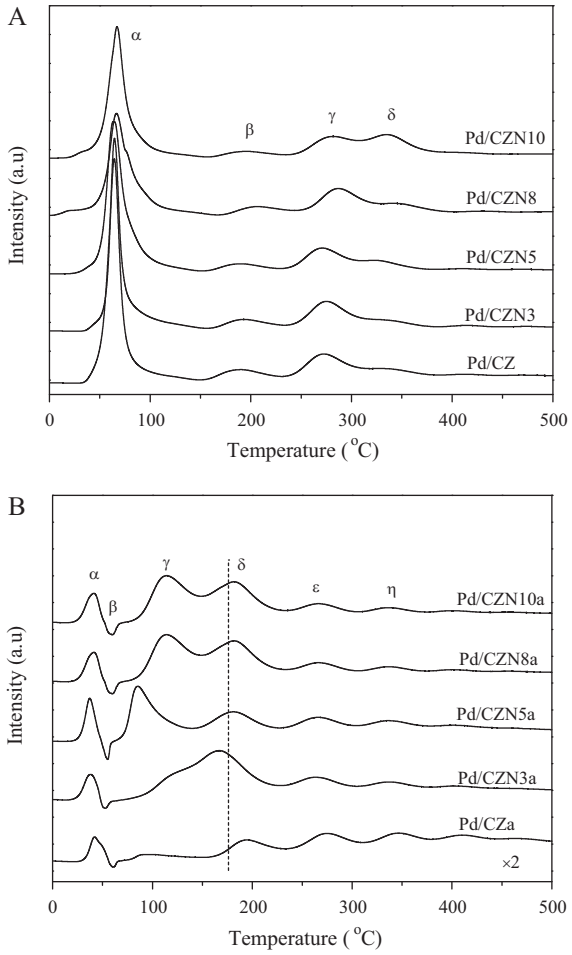

Fig. 6. TPR traces for the fresh and aged catalysts.

observed over a standard CuO sample in similar TPR procedures, it is convinced that the total amount of the H_2 consumption for peak α is too large to be reasonably attributed to the reduction of noble metal oxides absolutely, indicating the back-spillover of the oxygen process from the support to the PdO surface [54,55]. For instance, the H_2 consumption for theoretical PdO is just 41 μmol/gcat, while that for peak α in the case of Pd/CZ is 423 μmol/gcat. Summarily, we can conclude that there is a strong interaction between PdO and the support. With regard to Pd/CZN5, the H_2 consumption for peak α is 799 μmol/gcat, showing the increased SMSI due to the addition of Nd. It is worthwhile to note that the temperature of peak α over fresh samples slightly shifts towards lower temperature as the neodymia content in the mixed oxides increases, and further increase of neodymia content from 5wt.% to 10 wt.% does not further modify the TPR profiles. The similar behavior also occurs in the case of fresh supports. This observation indicates that Nd modified support with 5 wt.% content exhibits the best reducibility and the metal-support interaction between CZN5 and active PdO is the strongest.

In the case of aged catalysts (as shown in Fig. 6B), the intensity of peak α decreases obviously after calcination at 1100 °C. Papavasiliou et al. [7] have reported that the fresh three-way catalysts prepared by wet impregnation method shows high noble metal dispersion values, and a strong reduction of dispersion takes place after thermal aging. Therefore, the decrease of peak α intensity could be attributed to the agglomeration of PdO particles, that is to say, the decrease of PdO dispersion. The negative peak at ca.60 °C (peak β) is generally attributed to the decomposition of palladium hydride formed following PdO reduction. Peak γ is suggested to the reduction of stable PdO formed on the interaction between PdO and the support [56,57]. In the case of Pd/CZa, the absence of peak γ indicates the obvious sintering of active metal oxide for Pd/CZa. Interestingly, the area of peak γ increases due to the appearance of neodymia, proving that the addition of Nd could stabilize the PdO active species due to the increased strong metal-support interaction mentioned above. Peaks δ, ε and η are also suggested to the reduction of surface/subsurface oxygen from the support. Similarly to the fresh catalysts, Pd/CZN5a also shows the lowest temperature for PdO reduction.

In the analysis of catalytic performance (Section 3.1), it has been shown that the introduction of Nd is beneficial to the conversion of NO_x. Vidmar et al. [58] and Ranga Rao et al. [59] have proposed that the oxygen vacancies associated with the Ce^{3+} ions near the noble metal particles in CZ-supported catalysts are the active sites for NO_x activation. Therefore, we can conclude that the higher OSC caused by Nd doping is one of the main reasons for the enhanced catalytic conversion of NO_x. Among the aged catalysts, Pd/CZN5a exhibits the best reducibility and the strongest SMSI, leading to the relatively higher catalytic activity than other aged catalysts. Most importantly, the increased OSC results in the enlarged operation window, indicating the high catalytic efficiency of the modified catalysts.

4. Conclusion

In summary, the following conclusions can be put forward in view of the analysis mentioned above: (1) the addition of Nd into CZ leads to the formation of ceria–zirconia–neodymia (CZN) ternary solid solution, which shows the enhanced textural/structural properties. (2) Combined with the results of XRD and XPS, it can be inferred that Zr is substituted by the doped Nd in the framework of CZN solid solution, and Nd would migrate from bulk to the surface during high temperature aging. (3) The better reducibility and higher OSC as well as increased strong metal-support interaction caused by Nd addition are the main reason for the improved three-way catalytic activity and enlarged air/fuel operation window. (4) The modified solid solution with 5 wt.% neodymia shows the relatively better textural and structural properties considering that the capacity of foreign cation is limited in the crystal lattice of ceria–zirconia solid solution, and Pd/CZN5 shows the optimum three-way catalytic performance, especially for the corresponding aged one.

Acknowledgements

The authors acknowledge the Ministry of Science and Technology of China for the financial support of Project 2009AA064804 and the Science and Technology Department of Zhejiang Province for the financial support of Project 2009R50020. Moreover, the authors also grateful to Prof. Meiqing Shen at Key Laboratory for Green Chemical Technology of State Education Ministry, School of Chemical Engineering & Technology, Tianjin University for the dynamic oxygen storage capacity experiment.

References

[1] H. Birgersson, L. Eriksson, M. Boutonnet, S.G. Järås, Thermal gas treatment to regenerate spent automotive three-way exhaust gas catalysts (TWC), Appl. Catal. B: Environ. 54 (2004) 193–200.
[2] L.N. Ikryannikova, A.A. Aksenov, G.L. Markaryan, G.P. Murav'eva, B.G. Kostyuk, A.N. Kharlanov, E.V. Lunina, The red-ox treatment influence on the structure and properties of M_2O_3–CeO_2–ZrO_2 (M = Y, La) solid solutions, Appl. Catal. A: Gen. 210 (2001) 225–235.
[3] A. Martínez-Arías, M. Fernández-García, A.B. Hungría, A. Iglesias-Juez, K. Duncan, R. Smith, J.A. Anderson, J.C. Conesa, J. Soria, Effect of thermal sintering on light-off performance of Pd/(Ce, Zr)O_x/Al_2O_3 three-way catalysts: model gas and engine tests, J. Catal. 204 (2001) 238–248.

[4] B. Yue, R. Zhou, Y. Wang, X. Zheng, Study of the methane combustion and TPR/TPO properties of Pd/Ce–Zr–M/Al_2O_3 catalysts with M = Mg, Ca, Sr, Ba, J. Mol. Catal. A: Chem. 238 (2005) 241–249.

[5] X. Courtois, V. Perrichon, Distinct roles of copper in bimetallic copper–rhodium three-way catalysts deposited on redox supports, Appl. Catal. B: Environ. 57 (2005) 63–72.

[6] F. Dong, T. Tanabe, A. Suda, N. Takahashi, H. Sobukawa, H. Shinjoh, Investigation of the OSC performance of Pt/CeO_2–ZrO_2–Y_2O_3 catalysts by CO oxidation and $^{18}O/^{16}O$ isotopic exchange reaction, Chem. Eng. Sci. 63 (2008) 5020–5027.

[7] A. Papavasiliou, A. Tsetsekou, V. Matsouka, M. Konsolakis, I.V. Yentekakis, N. Boukos, Development of a Ce–Zr–La modified Pt/γ-Al_2O_3 TWCs' washcoat: effect of synthesis procedure on catalytic behavior and thermal durability, Appl. Catal. B: Environ. 90 (2009) 162–174.

[8] R.S. Monteiro, L.C. Dieguez, M. Schmal, The role of Pd precursors in the oxidation of carbon monoxide over Pd/Al_2O_3 and Pd/CeO_2/Al_2O_3 catalysts, Catal. Today 65 (2001) 77–89.

[9] J. Kašpar, P. Fornasiero, N. Hickey, Automotive catalytic converters: current status and some perspective, Catal. Today 77 (2003) 419–449.

[10] P. Fonasiero, R. Di Monte, G. Ranga Rao, J. Kašpar, S. Meriani, A. Trovarelli, M. Graziani, Rh-loaded CeO_2–ZrO_2 solid-solutions as highly efficient oxygen exchangers: dependence of the reduction behavior and the oxygen storage capacity on the structural-properties, J. Catal. 151 (1995) 168–177.

[11] J.R. González-Velasco, M.A. Gutiérrez-Ortiz, J.L. Marc, J.A. Botas, M. Pilar González-Marcos, G. Blanchard, Effects of redox thermal treatments and feed-stream composition on the activity of Ce/Zr mixed oxides for TWC applications, Appl. Catal. B: Environ. 25 (2000) 19–29.

[12] H. Vidal, J. Kašpar, M. Pijolat, G. Colon, S. Bernal, A. Cordón, V. Perrichon, F. Fally, Redox behavior of CeO_2–ZrO_2 mixed oxides. II. Influence of redox treatments on low surface area catalysts, Appl. Catal. B: Environ. 30 (2001) 75–85.

[13] Y. Nagai, T. Yamamoto, T. Tanaka, S. Yoshida, T. Nonaka, T. Okamoto, A. Suda, M. Sugiura, X-ray absorption fine structure analysis of local structure of CeO_2–ZrO_2 mixed oxides with the same composition ratio (Ce/Zr = 1), Catal. Today 74 (2002) 225–234.

[14] J.R. Kim, W.J. Myeong, S.K. Ihm, Characteristics in oxygen storage capacity of ceria–zirconia mixed oxides prepared by continuous hydrothermal synthesis in supercritical water, Appl. Catal. B: Environ. 71 (2007) 57–63.

[15] N. Le Phuc, E.C. Corbos, X. Courtois, F. Can, P. Marecot, D. Duprez, NO_x storage and reduction properties of Pt/$Ce_xZr_{1-x}O_2$ mixed oxides: sulfur resistance and regeneration, and ammonia formation, Appl. Catal. B: Environ. 93 (2009) 12–21.

[16] G. Li, Q. Wang, B. Zhao, R. Zhou, Modification of $Ce_{0.67}Zr_{0.33}O_2$ mixed oxides by coprecipitated/impregnated Co: effect on the surface and catalytic behavior of Pd only three-way catalyst, J. Mol. Catal. A: Chem. 326 (2010) 69–74.

[17] C. Larese, M. López Granados, R. Mariscal, J.L.G. Fierro, P.S. Lambrou, A.M. Efstathiou, The effect of calcination temperature on the oxygen storage and release properties of CeO_2 and Ce–Zr–O metal oxides modified by phosphorus incorporation, Appl. Catal. B: Environ. 59 (2005) 13–25.

[18] M. Zhao, M. Shen, J. Wang, Effect of surface area and bulk structure on oxygen storage capacity of $Ce_{0.67}Zr_{0.33}O_2$, J. Catal. 248 (2007) 258–267.

[19] A. Morikawa, T. Suzuki, T. Kanazawa, K. Kikuta, A. Suda, H. Shinjo, A new concept in high performance ceria–zirconia oxygen storage capacity material with Al_2O_3 as a diffusion barrier, Appl. Catal. B: Environ. 78 (2008) 210–221.

[20] M.V. Twigg, Progress and future challenges in controlling automotive exhaust gas emissions, Appl. Catal. B: Environ. 70 (2007) 2–15.

[21] S. Suhonen, M. Valden, M. Hietikko, R. Laitinen, A. Savimäki, M. Härkönen, Effect of Ce–Zr mixed oxides on the chemical state of Rh in alumina supported automotive exhaust catalysts studied by XPS and XRD, Appl. Catal. A: Gen. 218 (2008) 151–160.

[22] X. Wang, R.J. Gorte, J.P. Wagner, Deactivation mechanisms for Pd/ceria during the water–gas-shift reaction, J. Catal. 212 (2002) 225–230.

[23] A.I. Kozlov, D.H. Kim, A. Yezerets, P. Andersen, H.H. Kung, M.C. Kung, Effect of preparation method and redox treatment on the reducibility and structure of supported ceria–zirconia mixed oxide, J. Catal. 209 (2002) 417–426.

[24] V.R. Mastelaro, V. Briois, D.P.F. de Souza, C.L. Silva, Structure studies of a ZrO_2–CeO_2 doped system, J. Eur. Ceram. Soc. 23 (2003) 273–282.

[25] C. Larese, F. Cabello Galisteo, M. López Granados, R. Mariscal, J.L.G. Fierro, P.S. Lambrou, A.M. Efstathiou, Effects of the $CePO_4$ on the oxygen storage and release properties of CeO_2 and $Ce_{0.8}Zr_{0.2}O_2$ solid solution, J. Catal. 226 (2004) 443–456.

[26] A. Morikawa, K. Kikuta, A. Suda, H. Shinjo, Enhancement of oxygen storage capacity by reductive treatment of Al_2O_3 and CeO_2–ZrO_2 solid solution nanocomposite, Appl. Catal. B: Environ. 88 (2009) 542–549.

[27] J.D. Lin, J.G. Duh, Correlation of mechanical properties and composition in tetragonal CeO_2–Y_2O_3–ZrO_2 ceramic system, Mater. Chem. Phys. 78 (2002) 246–252.

[28] X. Wu, X. Wu, Q. Liang, J. Fan, D. Weng, Z. Xie, S. Wei, Structure and oxygen storage capacity of Pr/Nd doped CeO_2–ZrO_2 mixed oxides, Solid State Sci. 9 (2007) 636–643.

[29] E.V. Frolova, M. Ivanovskaya, V. Sadykov, G. Alikina, A. Lukashevich, S. Neophytides, Properties of Ce–Zr–La–O nano-system with ruthenium modified surface, Prog. Solid State Chem. 33 (2005) 317–325.

[30] J. Mikulova, S. Rossignol, F. Gérard, D. Mesnard, C. Kappenstein, D. Duprez, Properties of cerium–zirconium mixed oxides partially substituted by neodymium: comparison with Zr–Ce–Pr–O ternary oxides, J. Solid State Chem. 179 (2006) 2511–2520.

[31] Q. Wang, B. Zhao, G. Li, R. Zhou, Application of rare earth modified Zr-based ceria–zirconia solid solution in tree-way catalysts for automotive emission control, Environ. Sci. Technol. 44 (2010) 3870–3875.

[32] Q. Wang, G. Li, B. Zhao, M. Shen, R. Zhou, The effect of La doping on the structure of $Ce_{0.2}Zr_{0.8}O_2$ and the catalytic performance of its supported Pd-only three-way catalyst, Appl. Catal. B: Environ. 101 (2010) 150–159.

[33] J. Wang, M. Shen, Y. An, J. Wang, Ce–Zr–Sr mixed oxide prepared by the reversed microemulsion method for improved Pd-only three-way catalysts, Catal. Commun. 10 (2008) 103–107.

[34] N. Macleod, J. Isaac, R.M. Lambert, A comparison of sodium-modified Rh/γ-Al_2O_3 and Pd/γ-Al_2O_3 catalysts operated under simulated TWC conditions, Appl. Catal. B: Environ. 33 (2001) 335–343.

[35] I. Heo, J.W. Choung, P.S. Kim, I.-S. Nam, Y.I. Song, C.B. In, G.K. Yeo, The alteration of the performance of field-aged Pd-based TWCs towards CO and C_3H_6 oxidation, Appl. Catal. B: Environ. 92 (2009) 114–125.

[36] J. Kimpton, T.H. Randle, J. Drennan, Investigation of electrical conductivity as a function of dopant-ion radius in the systems $Zr_{0.75}Ce_{0.08}M_{0.17}O_{1.92}$ (M = Nd, Sm, Gd, Dy, Ho, Y, Er, Yb, Sc), Solid State Ionics 149 (2002) 89–98.

[37] J. Guo, D. Wu, L. Zhang, M. Gong, M. Zhao, Y. Chen, Preparation of nanometric CeO_2–ZrO_2–Nd_2O_3 solid solution and its catalytic performances, J. Alloys Compd. 460 (2008) 485–490.

[38] J. Fan, X. Wu, X. Wu, Q. Liang, R. Ran, D. Weng, Thermal ageing of Pt on low-surface-area CeO_2–ZrO_2–La_2O_3 mixed oxides: effect on the OSC performance, Appl. Catal. B: Environ. 81 (2008) 38–48.

[39] F.B. Noronha, E.C. Fendley, R.R. Soares, W.E. Alvarez, D.E. Resasco, Correlation between catalytic activity and support reducibility in the CO_2 reforming of methane over Pt/$Ce_xZr_{1-x}O_2$ catalysts, Chem. Eng. J. 82 (2001) 21–31.

[40] J. Fan, D. Weng, X. Wu, X. Wu, R. Ran, Modification of CeO_2–ZrO_2 mixed oxides by coprecipitated/impregnated Sr: effect on the microstructure and oxygen storage capacity, J. Catal. 258 (2008) 177–186.

[41] C. Bozo, N. Guilhaume, J.-M. Herrmann, Role of the ceria–zirconia support in the reactivity of platinum and palladium catalysts for methane total oxidation under lean conditions, J. Catal. 203 (2001) 393–406.

[42] P. Fornasiero, J. Kašpar, M. Graziani, On the rate determining step in the reduction of CeO_2–ZrO_2 mixed oxides, Appl. Catal. B: Environ. 22 (1999) L11–L14.

[43] H. Vidal, J. Kašpar, M. Pijolat, G. Colon, S. Bernal, A. Cordón, V. Perrichon, F. Fally, Redox behavior of CeO_2–ZrO_2 mixed oxides. I. Influence of redox treatments on high surface area catalysts, Appl. Catal. B: Environ. 27 (2000) 49–63.

[44] M. Boaro, F. Giordano, S. Recchia, V.D. Santo, M. Giona, A. Trovarellia, On the mechanism of fast oxygen storage and release in ceria–zirconia model catalysts, Appl. Catal. B: Environ. 52 (2004) 225–237.

[45] F. Dong, A. Suda, T. Tanabe, Dynamic oxygen mobility and a new insight into the role of Zr atoms in three-way catalysts of Pt/CeO_2–ZrO_2, Catal. Today 93–95 (2004) 827–832.

[46] Q. Wang, G. Li, B. Zhao, R. Zhou, Synthesis of La modified ceria–zirconia solid solution by advanced supercritical ethanol drying technology and its application in Pd-only three-way catalyst, Appl. Catal. B: Environ. 100 (2010) 516–528.

[47] S. Salasc, V. Perrichon, M. Perrichon, M. Primet, N. Mouaddib-Moral, Titration by oxygen of the spill-over hydrogen adsorbed on ceria–zirconia supported palladium–rhodium catalysts, J. Catal. 206 (2002) 82–90.

[48] W. Lin, Y.X. Zhu, N.Z. Wu, Y.C. Xie, I. Murwani, E. Kemnitz, Total oxidation of methane at low temperature over Pd/TiO_2/Al_2O_3: effects of the support and residual chlorine ions, Appl. Catal. B: Environ. 50 (2004) 59–66.

[49] M.P. Yeste, J.C. Hernández, S. Bernal, G. Blanco, J.J. Calvino, J.A. Pérez-Omil, J.M. Pintado, Comparative study of the reducibility under H_2 and CO of two thermally aged $Ce_{0.62}Zr_{0.38}O_2$ mixed oxide samples, Catal. Today 141 (2009) 409–414.

[50] J. Kašpar, P. Fornasiero, M. Graziani, Use of CeO_2-based oxides in the three-way catalysis, Catal. Today 50 (1999) 285–298.

[51] I. Atribak, A. Bueno-López, A. García-García, Combined removal of diesel soot particulates and NO_x over CeO_2–ZrO_2 mixed oxides, J. Catal. 259 (2008) 123–132.

[52] R.A. Daley, S.Y. Christou, A.M. Efstathiou, J.A. Anderson, Influence of oxychlorination treatments on the redox and oxygen storage and release properties of thermally aged Pd–Rh/$Ce_xZr_{1-x}O_2$/Al_2O_3 model three-way catalysts, Appl. Catal. B: Environ. 60 (2005) 117–127.

[53] N. Hickey, P. Fornasiero, J. Kašpar, J.M. Gatica, S. Bernal, Effects of the nature of the reducing agent on the transient redox behavior of NM/$Ce_{0.68}Zr_{0.32}O_2$ (NM = Pt, Pd, and Rh), J. Catal. 200 (2001) 181–193.

[54] S.Y. Christou, C.N. Costa, A.M. Efstathiou, A two-step reaction mechanism of oxygen release from Pd/CeO_2: mathematical modelling based on step gas concentration experiments, Top. Catal. 30/31 (2004) 325–331.

[55] C.N. Costa, S.Y. Christou, G. Georgiou, A.M. Efstathiou, Mathematical modeling of the oxygen storage capacity phenomenon studied by CO pulse transient experiments over Pd/CeO_2 catalyst, J. Catal. 219 (2003) 259–272.

[56] P.S. Lambrou, A.M. Efstathiou, The effects of Fe on the oxygen storage and release properties of model Pd–Rh/CeO_2–Al_2O_3 three-way catalyst, J. Catal. 240 (2006) 182–193.

[57] G. Li, B. Zhao, Q. Wang, R. Zhou, The effect of Ni on the structure and catalytic behavior of model Pd/$Ce_{0.67}Zr_{0.33}O_2$ three-way catalyst before and after aging, Appl. Catal. B: Environ. 97 (2010) 41–48.

[58] P. Vidmar, P. Fornasiero, J. Kašpar, M. Graziani, Effects of trivalent dopants on the redox properties of $Ce_{0.6}Zr_{0.4}O_2$ mixed oxide, J. Catal. 171 (1997) 160–168.

[59] G. Ranga Rao, P. Fornasiero, R. Di Monte, J. Kašpar, G. Vlaic, G. Balducci, S. Meriani, G. Gubitosa, A. Cremona, M. Graziani, Reduction of NO over partially reduced metal-loaded CeO_2–ZrO_2 solid solutions, J. Catal. 162 (1996) 1–9.